Perennial Snow and Ice Volumes on Iliamna Volcano, Alaska, Estimated With Ice Radar and Volume Modeling

Water-Resources Investigations Report 99-4176

U.S. Department of the Interior
U.S. Geological Survey

Cover: View of Iliamna Volcano from the Johnson River Valley.

Perennial Snow and Ice Volumes on Iliamna Volcano, Alaska, Estimated with Ice Radar and Volume Modeling

By Dennis C. Trabant

U.S. GEOLOGICAL SURVEY

Water-Resources Investigations Report 99-4176

Anchorage, Alaska
1999

U.S. DEPARTMENT OF THE INTERIOR
BRUCE BABBITT, Secretary

U.S. GEOLOGICAL SURVEY
Charles G. Groat, Director

For additional information:

District Chief
U.S. Geological Survey
4230 University Drive, Suite 201
Anchorage, AK 99508-4664

http://ak.water.usgs.gov

Copies of this report may be purchased from:

U.S. Geological Survey
Branch of Information Services
Box 25286
Denver, CO 80225-0286

CONTENTS

FIGURES

TABLES

CONVERSION FACTORS AND VERTICAL DATUM

Multiply	by	To obtain
meter (m)	3.281	foot
kilometer (km)	0.6214	mile
square meter (m^2)	10.76	square foot
cubic kilometer (km^3)	0.2399	cubic mile
meter per microsecond (m/µs)	3.281	foot per microsecond

Sea level: In this report, “sea level” refers to the National Geodetic Vertical Datum of 1929—A geodetic datum derived from a general adjustment of the first-order level nets of the United States and Canada, formerly called Sea Level Datum of 1929.

Perennial Snow and Ice Volumes on Iliamna Volcano, Alaska, Estimated With Ice Radar and Volume Modeling

by Dennis C. Trabant

ABSTRACT

The volume of four of the largest glaciers on Iliamna Volcano was estimated using the volume model developed for evaluating glacier volumes on Redoubt Volcano. The volume model is controlled by simulated valley cross sections that are constructed by fitting third-order polynomials to the shape of the valley walls exposed above the glacier surface. Critical cross sections were field checked by sounding with ice-penetrating radar during July 1998. The estimated volumes of perennial snow and glacier ice for Tuxedni, Lateral, Red, and Umbrella Glaciers are 8.6, 0.85, 4.7, and 0.60 cubic kilometers respectively. The estimated volume of snow and ice on the upper 1,000 meters of the volcano is about 1 cubic kilometer. The volume estimates are thought to have errors of no more than ±25 percent. The volumes estimated for the four largest glaciers are more than three times the total volume of snow and ice on Mount Rainier and about 82 times the total volume of snow and ice that was on Mount St. Helens before its May 18, 1980 eruption. Volcanoes mantled by substantial snow and ice covers have produced the largest and most catastrophic lahars and floods. Therefore, it is prudent to expect that, during an eruptive episode, flooding and lahars threaten all of the drainages heading on Iliamna Volcano. On the other hand, debris avalanches can happen any time. Fortunately, their influence is generally limited to the area within a few kilometers of the summit.

INTRODUCTION

Location and Description

Iliamna Volcano is near the northeastern end of the Aleutian volcanic arc, on the west side of Cook Inlet, about 225 km southwest of Anchorage, Alaska (fig. 1) in Lake Clark National Park. The volcano is a broad, roughly cone-shaped composite stratovolcano with a summit altitude of 3,053 m. Most of the volcano is covered by perennial snow and glacier ice. The broad base, below about 1,000-m altitude, is deeply dissected by glacier erosion, which has produced steep, 600-m-high headwalls along the southern and eastern flanks extending nearly to the summit. Since the last eruption, large debris avalanches have begun as mass failures of the highly altered rock on the steep upper 2,000 m of the massif. A snow, ice, and rock avalanche in 1994 was recorded on regional seismometers as far away as 150 km. Runout deposits extended to 10 km and were primarily snow and ice with minor amounts of rock.

Eruption History

Iliamna Volcano has had no well-documented eruptions during the last 200 years. However, active fumaroles near the summit inspire a continuing series of eruption reports dating back to 1867 (Coats, 1950; Miller and

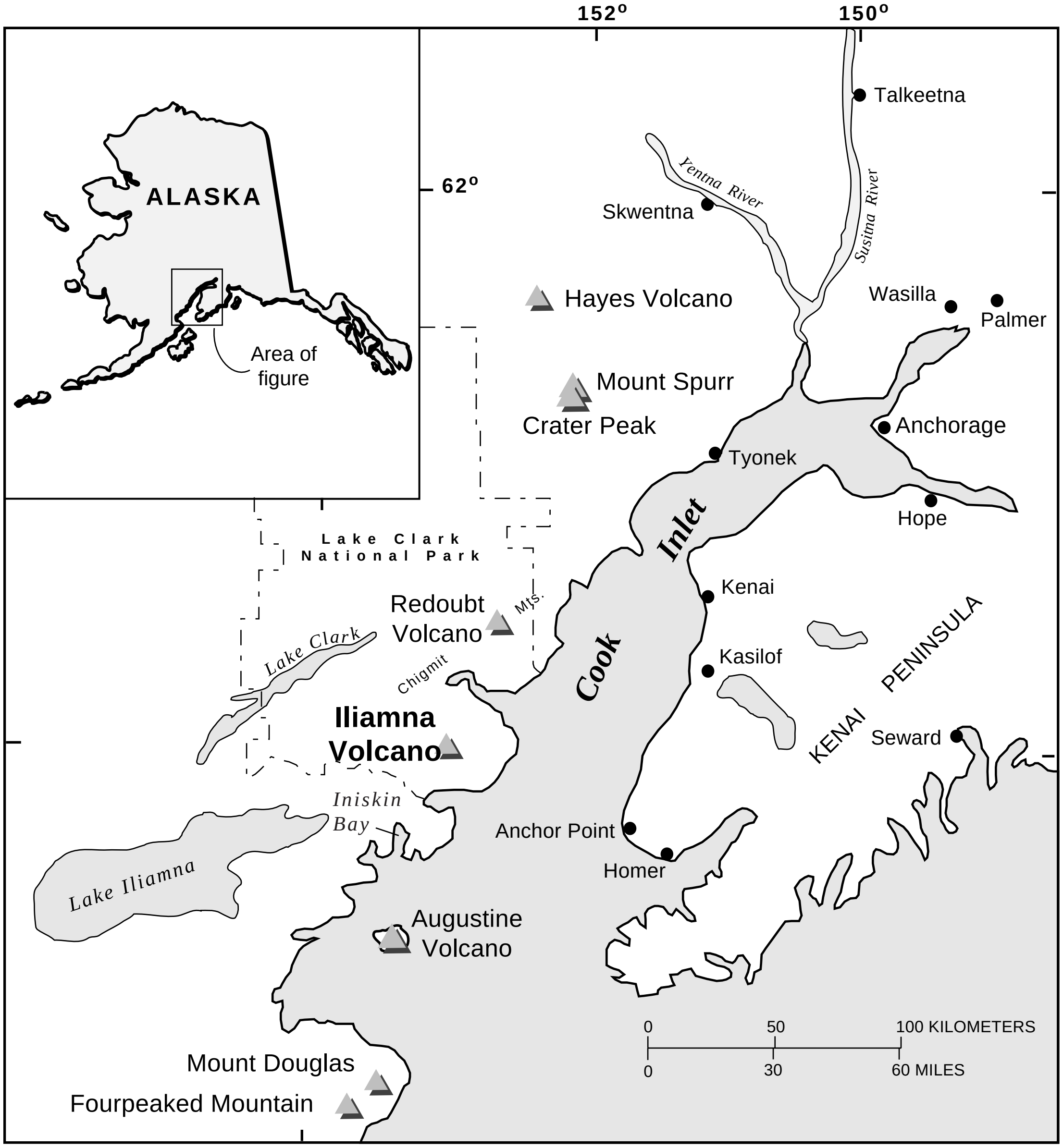

Figure 1. Location of Iliamna Volcano and other volcanoes near Cook Inlet, Alaska.

others, 1998). The most recent eruption has been dated at about 300 years BP (Begét, 1996). However, two strong seismic swarms recorded beneath the volcano during 1996 (Neal and McGimsey, 1997) indicate that Iliamna Volcano is dormant, not extinct.

Purpose and Scope

The purpose of this study was to evaluate the volume of the major glaciers on Iliamna Volcano for use in assessments of the hazards associated with pyroclastic eruptions. The four largest glaciers on Iliamna were chosen for analysis. They are Tuxedni, Lateral, Red, and Umbrella Glaciers (fig. 2). These glaciers are the sources of the largest drainages on the north, east, and southwest sides of the volcano. The volume and area of each glacier were subdivided at about the 1,000-m surface altitude contour (fig. 2) because the snow and ice above and below about 1,000-m altitude constitute different hazards. The snow and ice on the steep upper cone of Iliamna Volcano above 1,000 m may be completely removed by even a relatively small eruption. Below 1,000-m altitude, the glaciers will probably lose little mass during an eruption similar to the glaciers that were measured during the 1989-90 eruptions of Redoubt Volcano (Trabant, 1997; Trabant and others, 1994). Only a plinian eruption is likely to disrupt all of the glacier ice on Iliamna Volcano. No previous evaluation has been made of the surface area or volume distribution of perennial snow and glacier ice on Iliamna Volcano.

GLACIER-VOLUME MODEL

Glacier volumes were determined by volume modeling and were field checked by glacier-thickness measurements at 11 locations. The volume-modeling scheme was developed for an assessment of the ice volume on Redoubt Volcano (fig. 1) (Trabant, 1997). The model evaluates the volume of a glacier by “subtracting” a simulated glacier-bed surface from the mapped, upper surface of the glacier. Digital surfaces were prepared and the differences evaluated using Quicksurf, an application supported by AutoCAD, which uses the triangulated irregular network (TIN) method. Prismoidal volumes were calculated from the digital surfaces.

The upper surface of each glacier was defined by a digital elevation model (DEM) created by U.S. Geological Survey, EROS Data Center, Anchorage from 1:250,000 scale maps based on aerial photography spanning from 1950 to 1966. Glacier termini on these maps were updated from 1977 and 1980 aerial photography.

The beds of the glaciers were simulated by fitting third-order polynomial curves to the parts of the valley walls that are exposed above the glaciers (fig. 3). Cross sections were located where the greatest quantity of ice was expected and where the slopes of the valley walls were continuous and paired across the glacier, thus producing well-controlled simulations. The density of cross sections was guided by the experience gained during the analysis of the ice volumes on Redoubt Volcano (Trabant, 1997). The glacier thicknesses that were predicted by the simulated cross sections were checked in the field before the ice-volume modeling phase of the analysis.

The bottom surfaces of the glaciers were modeled by incorporating the measured glacier thicknesses (fig. 4) in the cross-section simulations and re-fitting the third-degree polynomial curves. The sub-glacial parts of the new cross sections were plotted in a three-dimensional volume model and linear interpolations were made between the cross-section nodes (fig. 3). Non-linear extrapolations were made into small tributaries and to the glacier edges above and below the highest and lowest simulated cross sections. Glacier thickness estimates for the non-linear extrapolations were bounded by a maximum equal to the nearest simulated thickness and zero in the case of glacier edges or by a maximum of a few tens of meters where glacier edges were at high-altitude passes. All of the points and the three-dimensional glacier boundaries shown in figure 3 are the basis for the model of the glacier bed surface.

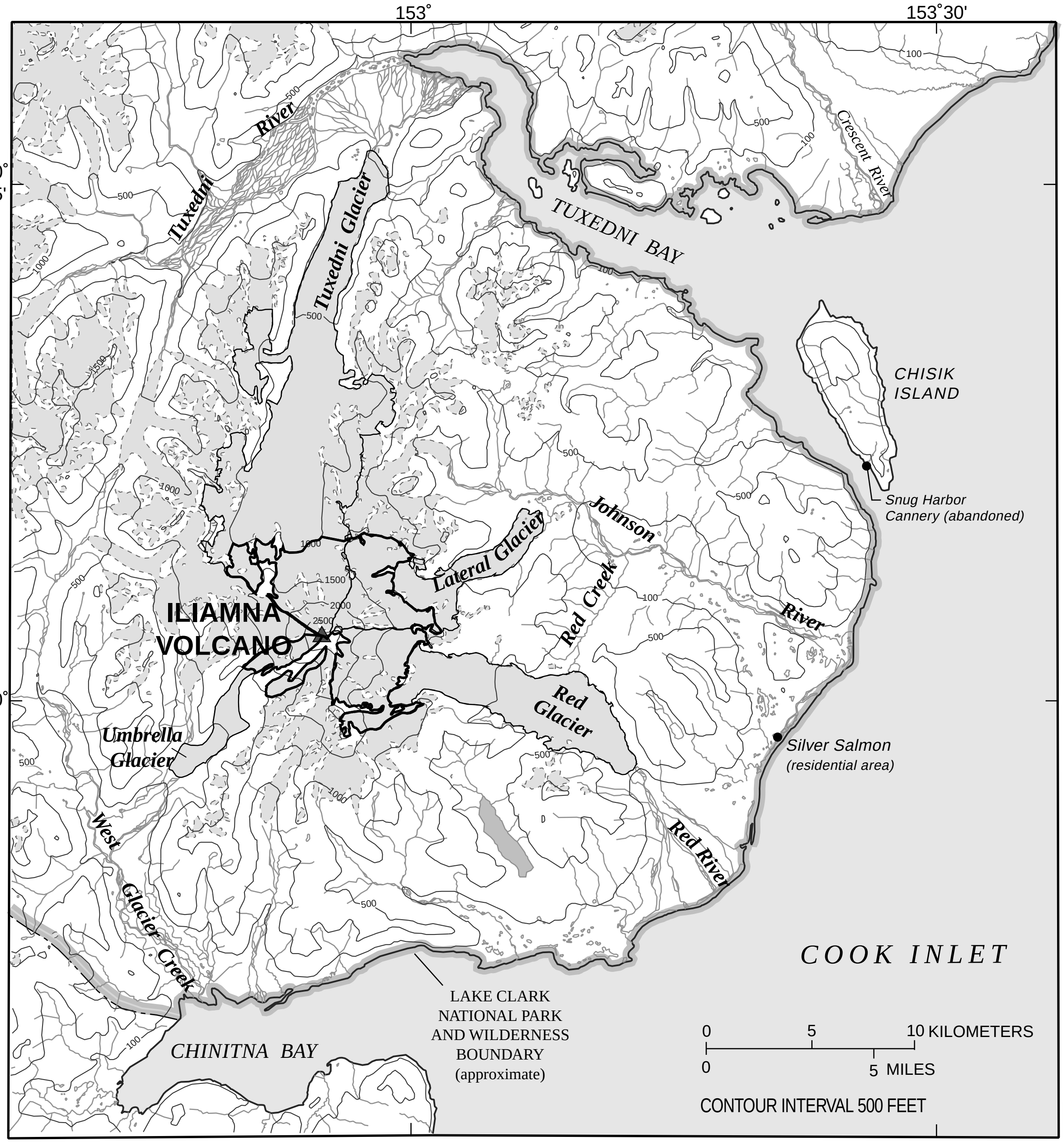

Figure 2. Topographic map of Iliamna Volcano with the edges of Tuxedni, Lateral, Red, and Umbrella Glaciers emphasized. (The glacier area on summit cone above 1000-m altitude is inside the heavy line.)

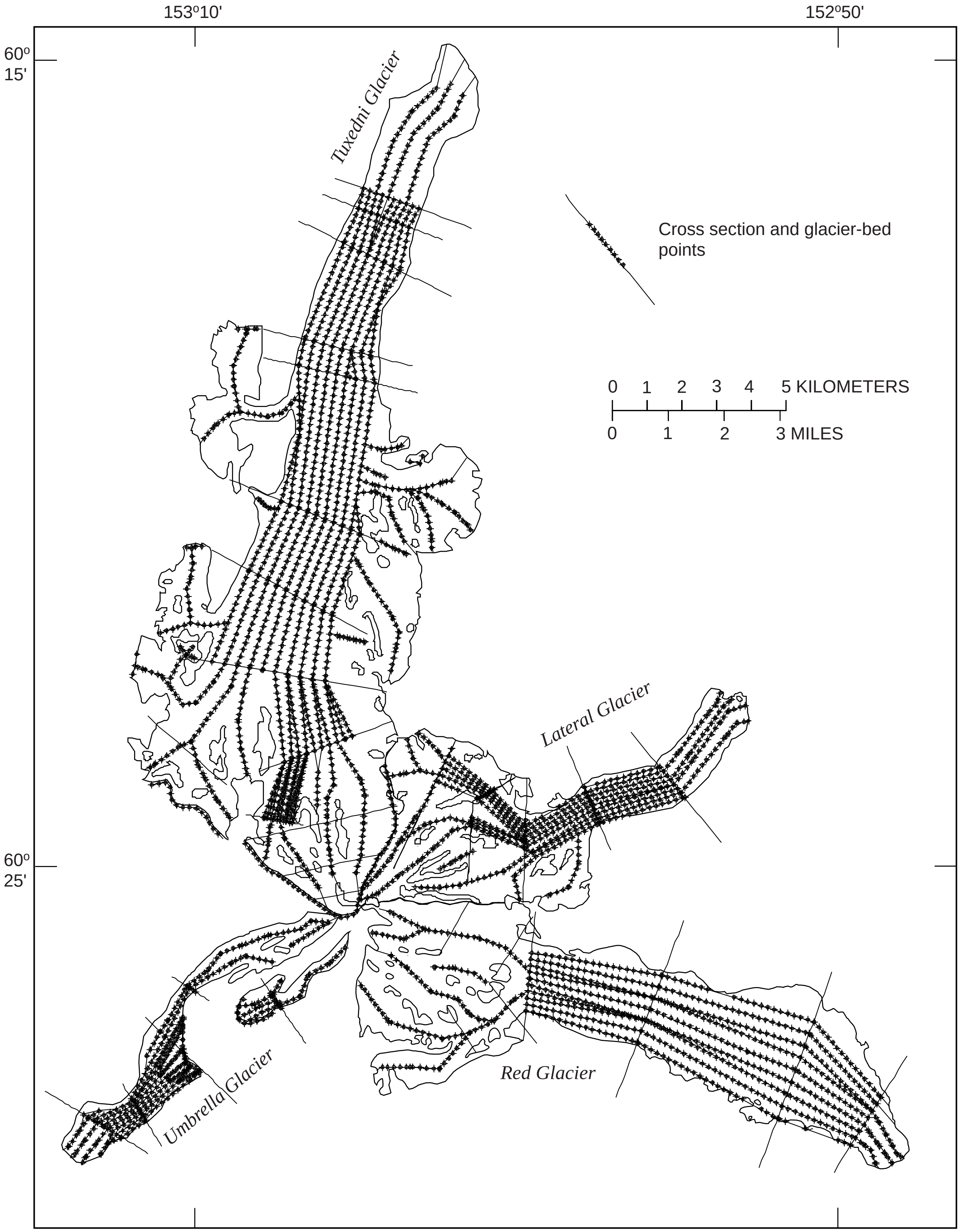

Figure 3. Cross section locations of the four largest glaciers on Iliamna Volcano. (All glacier-bed points and the three-dimensional glacier boundary were used for creating the glacier-bed model.)

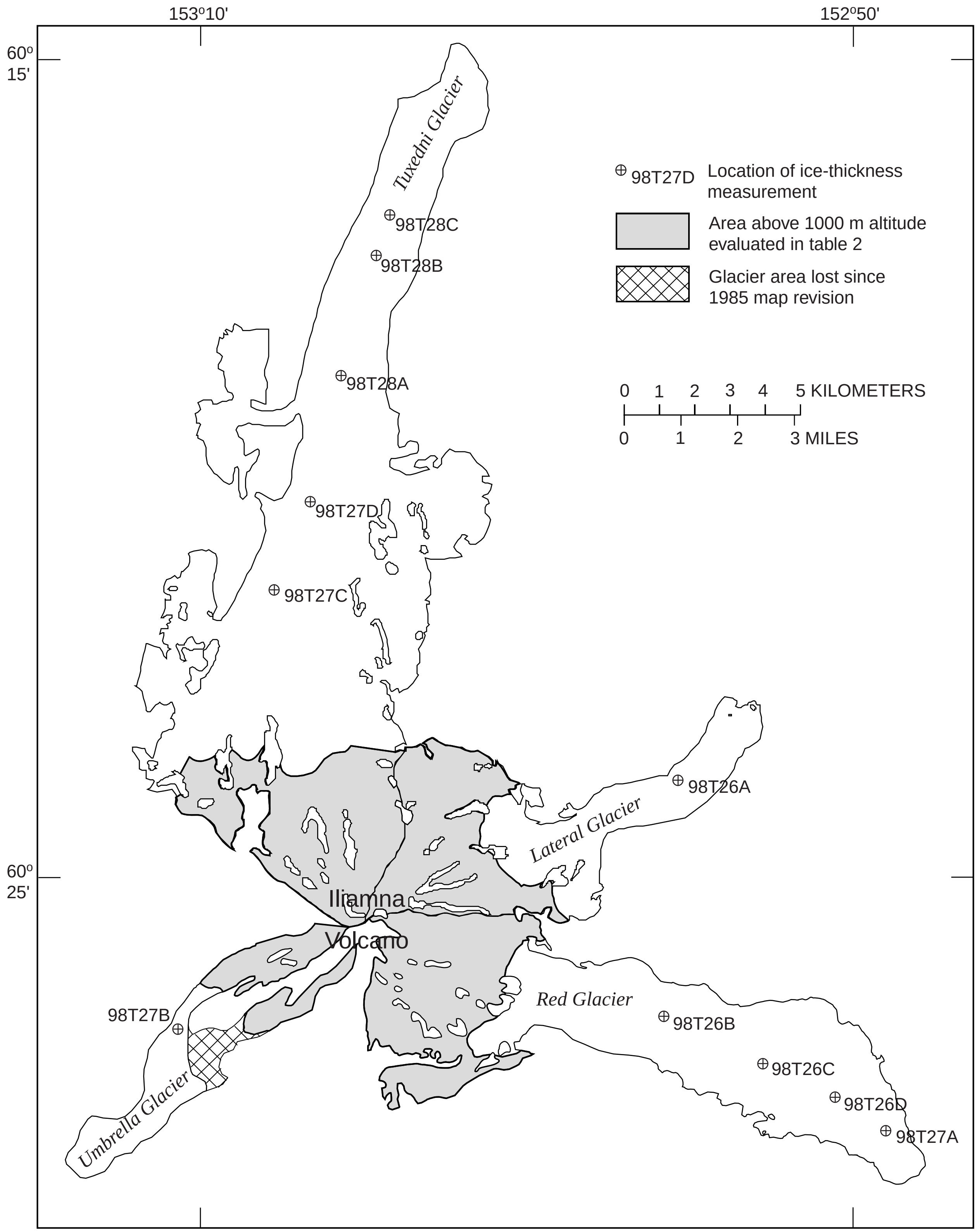

Figure 4. Tuxedni, Lateral, Red, and Umbrella Glacier edges as shown on the 1985 revision of the 1957 U.S. Geological Survey map. (See table 1 for ice-thickness data. See table 2 for separately determined perennial snow and ice volume on the summit cone.)

The intrinsic error in extrapolating bed shape from valley walls was analyzed in a carefully controlled reach of Drift Glacier on Redoubt Volcano (Trabant, 1997). In that analysis, 20 cross sections were rearranged by four different schemes in the same 2.5-km reach and these results were compared with the volume resulting from four cross sections connected by linear interpolations. The conclusion was that the modeled bed shape constructed from the reduced number of cross sections and connected by linear interpolations introduced an uncertainty of no more than 7 percent into the final volume determination (Trabant, 1997). The average longitudinal separation between the cross sections at Iliamna Volcano was about twice that at Redoubt Volcano. Therefore, the error in the volume estimates associated with extrapolation of bed shape may be as large as ±15 percent.

FIELD OBSERVATIONS, DATA ANALYSIS, AND MEASUREMENT ERRORS

Glacier ice thickness was measured with ice-penetrating radar at 11 sites during July 1998 (fig. 4 and table 1). Ice-thickness data were gathered in a manner similar to that used at Redoubt Volcano (Trabant, 1997) and used to validate and correct the cross-section simulations. Evaluation of the simulated cross sections indicated that the simulated depth of the cross section near 98T26B on Red Glacier (table 1) was too shallow on the basis of surrounding simulated thicknesses, its central location in the longitudinal profile of the glacier, and the surface slope of the glacier. Therefore, it was the highest priority site for field checking. The field check revealed that the simulated thickness was about two-thirds of the measured thickness. The other simulated thicknesses averaged 102 percent of the measured thicknesses, ranging from 85 to 119 percent of the measured thicknesses.

In table 1, the *Separation* is the distance between the radar transmitter and the receiver. Separations were measured with the 30-m radar antennae half-lengths. The *Delay Time* was measured with a 50 MHz field-portable oscilloscope. The oscilloscope was triggered by the arrival of the airwave. The signal was digitally captured and 256 waveforms were averaged to eliminate random noise. The *Signal Quality* was subjectively judged in the field on the basis of the signal to noise ratio. A signal was judged to be poor (P) if the signal was two to three times larger than the noise level; good (G) if the signal was three to four times larger than the noise level; and excellent (E) if the signal was five or more times larger than the noise level. The *Measured Glacier Thickness* (h) was calculated from the separation distance (s), in meters, and delay time (t_d) assuming that the velocity of radio wave propagation in ice (v_i) is 168 m/µs and in air (v_a) is 299.7 m/µs by:

$$h = \frac{1}{2}\sqrt{v_i^2\left(t_d + \frac{s}{v_a}\right)^2 - s^2}$$

Field logistics made it possible to acquire a few additional depth soundings at locations between the pre-defined cross sections. Therefore, simulated glacier thicknesses are not available for all of the measured glacier thicknesses in table 1.

Recent thinning of the glaciers was noted during the July 1998 field visit. The most striking change was on Umbrella Glacier, where thinning had completely disconnected the southern tributary from the main branch. Estimated changes in the boundary of Umbrella Glacier are shown in figure 4. The other three glaciers were judged to be thinning in their lower reaches and approaching stagnation at their termini on the basis of the large number and large size of moulins, lack of crevassing, and relative depression of the debris-free ice upstream from the debris-covered termini. The debris-covered terminus of Red Glacier was

Table 1. Glacier thickness measurement locations, transmitter/receiver separations, reflected signal delay times, qualitative signal quality, and measured and simulated glacier thickness

[Midpoint locations for the radar system were estimated in the field and marked on field maps; µs, microsecond; qualitative signal quality: E excellent; G good; P poor; simulated glacier thicknesses were estimated prior to the field visit; NA, not applicable—thickness estimate was not made at this location prior to field visit]

Map ID (fig. 4)	Midpoint locations UTM coordinates (meters)		Transmitter/ receiver separation (meters)	Reflected signal delay time (µs)	Qualitative signal quality	Glacier thickness (meters)	
	E	N				Measured	Simulated
98T26A	504274	6658831	100	1.00	G	100	96
98T26B	503842	6652114	50	3.32	G	292	200[1]
98T26C	506671	6650817	50	2.84	E	251	NA
98T26D	508720	6649835	50	2.42	P	216	NA
98T27A	510122	6648924	45	2.34	G	208	239
98T27B	490091	6651798	50	1.72	E	157	NA
98T27C	492815	6664237	50	3.16	G	278	253
98T27D	493867	6666719	45	4.00	P	348	297
98T28A	494736	6670295	50	4.41	P	384	368
98T28B	495718	6673696	50	1.52	P	139	140
98T28C	496115	6674853	75	1.72	P	161	192

[1]Simulated glacier thickness was considered questionable before the fieldwork began.

especially notable for the almost impenetrable growth of brush on its surface, which suggests that there have been many years of near stagnation. Retreat of the termini since the maps were revised using 1977 and 1980 photography is judged to be small because a thick and continuous debris cover on the termini preserves glacier ice. Ice volumes were calculated relative to the mapped glacier surfaces and glacier edges except for Umbrella Glacier. This means that the calculated ice volumes are slightly too large near the termini. On the other hand, the volume modeling technique tends to underestimate glacier volume (Trabant, 1997), which somewhat compensates for the bias caused by glacier thinning since the maps were revised.

The measured glacier thicknesses in table 1 were calculated assuming that the radar reflection came from the glacier bed approximately under the antennae. Corrections for the slopes of the glaciers' surfaces and beds were not made because the corrections are usually smaller than other errors in the measurements and ignoring the correction does not introduce a bias (Trabant, 1997). Nevertheless, it is important to remember that radar thicknesses are minimum thicknesses, because the effective radius of the propagating wave front is large and a reflection comes from the first encounter with a surface capable of producing a coherent reflection.

The combined errors of oscilloscope sweep rate, oscilloscope reading, and glacier-density assumptions are assumed to be similar to those found at Redoubt Volcano (Trabant, 1997). Therefore, the measured thicknesses are assumed to have an uncertainty of ±6 percent. This error assessment is generous for the Iliamna data because the digitizing oscilloscope used at Iliamna supported waveform averaging and digital evaluation of delay times that should reduce reading errors compared with the unaveraged, analog oscilloscope used at Redoubt Volcano.

GLACIER VOLUMES ON ILIAMNA VOLCANO

The total perennial snow and ice volume in the four glaciers evaluated on Iliamna Volcano is 14.8 km^3. The estimated volumes and measured surface areas are summarized in table 2.

The volume of perennial snow and ice varies seasonally depending on the quantity lost by melting at low altitudes and the quantity gained as seasonal snow. However, on a year-to-year basis, the mass lost by melting at low altitudes is approximately equal to the mass of seasonal snow converted to perennial snow and ice at high altitudes. Excess accumulation at high altitudes is redistributed by glacier flow to the areas of excess melting at low altitudes, thereby maintaining the general shape of the glacier. Therefore, on a year-to-year basis, the distribution of glacier volume with altitude changes only slowly.

The error in the estimated glacier volumes may be as large as ±25 percent. The estimated glacier volumes above 1,000-m altitude are not well controlled by valley cross sections or ice-thickness measurements. However, the steep snow and ice surfaces naturally constrain ice-thickness maximums, which helps to limit the errors in volume estimation. The ±25 percent error is larger than the error of ± 20 percent that was assigned to the glacier volumes reported for Redoubt Volcano (Trabant, 1997) because the maps used to create the upper glacier surfaces on Redoubt Volcano had been compiled more recently and more accurately.

GLACIO-VOLCANIC HAZARDS

It is widely recognized that the most voluminous and catastrophic lahars and floods result from eruptions of volcanoes mantled by substantial snow and ice covers; even minor eruptions can be exacerbated when volcanic

Table 2. Glacier volumes and areas on Iliamna Volcano

[km^3, cubic kilometer; m^2, square meter]

	Tuxedni Glacier		Lateral Glacier		Red Glacier		Umbrella Glacier	
	Volume (km^3)	Area ($x10^6 m^2$)	Volume (km^3)	Area ($x10^6 m^2$)	Volume (km^3)	Area ($x10^6 m^2$)	Volume (km^3)	Area ($x10^6 m^2$)
Upper cone, above 1,000-m altitude	0.32	18.3	0.25	14.8	0.34	17.4	0.11	5.6
Total	8.6	107.7	0.85	30.3	4.7	52.5	0.6	12.3

products interact with snow and ice (Major and Newhall, 1989). The hydrologic and mass-failure hazards associated with glaciated volcanic terrain have been documented for the Cascade volcanoes (Scott, 1988; Scott and others, 1995). The devastating mudflows generated by the 1980 eruption of Mount St. Helens, in Washington State, emphasized the need for information about the volume and distribution of snow and ice on volcanoes (Driedger and Kennard, 1986). However, the relation between the volume distribution of perennial snow and ice, volcanic explosivity (Newhall and Self, 1982), and lahar and flood hazards is poorly defined in the scientific literature. Nevertheless, it is apparent that increasing the area covered by snow and ice generally increases the potential for initiating lahars and floods during eruptions. Rough snow and ice surfaces dramatically increase the potential for lahar and flood generation. On Redoubt Volcano, the glacier surface below the 1989-90 vent was a highly crevassed icefall. Most of the glacier ice in that reach was mechanically entrained by hot-rock avalanches, debris flows, and pyroclastic flows during the first eruptions (Trabant and others, 1994). These same flows largely overrode the smoother glacier surface and snow-covered areas below the icefall. In another example, it has been reported that lahars have traversed smooth snowfields incorporating only small quantities of the underlying snow (Suwa and Ohura, 1976).

Glaciers on active volcanoes supply water to the interior of the volcanic edifice, promoting hydrothermal alteration that weakens the rock and pyroclastic layers that form the volcano and increases the potential for steam explosions. Progressive weakening of rock and pyroclastic layers on steep slopes increases the potential for mass failures, especially where valleys are over-steepened by glacier and stream erosion and when stimulated by the seismic shaking associated with volcanic unrest. Debris flows from mass failures may extend more than 100 km down the surrounding drainages (Hoblitt and others, 1995). Furthermore, subsurface water in the volcanic edifice may interact with magma, significantly increasing the potential for explosive emissions (Mastin, 1995).

Jökulhlaups are sudden, sometimes catastrophic, releases of water from glaciers. Jökulhlaups may have surface or subglacial water sources. Volcanoes are especially prone to producing subglacial water bodies because changing heat flow to the base of glaciers may locally increase basal melting and sliding, particularly during precursory eruptive phases. Prediction of jökulhlaups, especially on poorly studied glacier-clad volcanoes, is difficult.

Seasonal snow increases the total volume of water available for interaction with eruptive products on volcanoes and in the surrounding valleys. For example, during the 1989-90 eruptions of Redoubt Volcano, pyroclastic flows and floods repeatedly swept the Drift River valley and incorporated the seasonal snow. The volume of seasonal snow entrained by the floods was estimated to be 35×10^6 m^3 of water equivalent, amounting to nearly 30 percent of the cumulative flow volume 22 km downstream from the volcano (Trabant and others, 1994).

The most far-reaching hazard associated with an explosive eruption of Iliamna Volcano is ash that could affect half of the State's population and disrupt transportation and communications in Anchorage and on the Kenai Peninsula. Airborne ash is an important hazard to local and international air traffic (Casadevall, 1994), and to oil tanker and freighter traffic in Cook Inlet. Eruption-related flooding and lahars threaten world-class sport-fishing areas, and tourist and guide businesses along the west coast of Cook Inlet near Iliamna Volcano.

CONCLUSIONS

The four measured glaciers on Iliamna Volcano have approximately three times the total volume of snow and ice on Mount Rainier and about 82 times the total volume of snow and ice that was on Mount St. Helens before its May 18, 1980 eruption. The geohydrologic hazards at volcanoes near Mount Rainier (Hoblitt and others, 1995; Scott and others, 1995) and Mount St. Helens (Wolfe and Pierson, 1995; Scott, 1988) are well documented. Projecting similar hazards in the major drainages around Iliamna Volcano is reasonable. For example, during the 1989-90 eruptions of Redoubt Volcano, flooding swept the entire valley of the Drift River and carried blocks of glacier ice and sediment into Cook Inlet, more than 22 km from the volcano (Trabant and Meyer, 1992).

REFERENCES CITED

Begét, J.E., 1996, Dendrochronologic, archeologic, and radiocarbon data on recent eruptions of Iliamna and Augustine Volcanoes, Alaska [abs]: Eos, Transactions, American Geophysical Union, v. 77, p. F814.

Casadevall, T.J., 1994, The 1989–1990 eruption of Redoubt Volcano, Alaska—Impacts on aircraft operations: Journal of Volcanology and Geothermal Research, v. 62, p. 301-316.

Coats, R.R., 1950, Volcanic activity in the Aleutian arc: U.S. Geological Survey Bulletin 974-B, p. 35-47.

Driedger, C.L., and Kennard, P.M., 1986, Ice volumes on Cascade Volcanoes—Mount Rainier, Mount Hood, Three Sisters, and Mount Shasta: U.S. Geological Survey Professional Paper 1365, 28 p.

Hoblitt, R.P., Walder, J.S., Driedger, C.L., Scott, K.M., Pringle, P.T., and Vallance, J.W., 1995, Volcano hazards from Mount Rainier, Washington: U.S. Geological Survey Open-File Report 95-273, 10 p.

Major, J.J., and Newhall, C.G., 1989, Snow and ice perturbation during historical volcanic eruptions and the formation of lahars and floods: Bulletin of Volcanology, v. 52, p. 1-27.

Mastin, L.G., 1995, Magma/water mixing in static and dynamically rising magma columns—A case study from Kilauea Volcano, Hawaii: Joint U.S. (NSF) / Japanese (JSCS) Conference on Intense Multiphase Interactions, Santa Barbara, California, June 9-13, 1995, Proceedings, p. 344-346.

Miller, T.P., McGimsey, R.G., Richter, D.H., Riehle, J.R., Nye, C.J., Yount, M.E., and Dumoulin, J.A., 1998, Catalog of historically active volcanoes of Alaska: U.S. Geological Survey Open-File Report 98-582, 104 p.

Neal, C.A., and McGimsey, R.G., 1997, 1996 volcanic activity in Alaska and Kamchatka—Summary of vents and response of the Alaska Volcano Observatory: U.S. Geological Survey Open-File Report 97-433, 41 p.

Newhall, C.G., and Self, S., 1982, The volcanic explosivity index (VEI)—An estimate of explosive magnitude for historical volcanism: Journal of Geophysical Research, v. 87, no. C2, p. 1231-1238.

Scott, K.M., 1988, Origins, behavior, and sedimentology of lahars and lahar-runout flows in the Toutle-Cowlitz River system: U.S. Geological Survey Professional Paper 1447-A, 76 p.

Scott, K.M., Vallance, J.W., and Pringle, P.T., 1995, Sedimentology, behavior, and hazards of debris flows at Mount Rainier, Washington: U.S. Geological Survey Professional Paper 1547, 56 p.

Suwa, A., and Ohura, E., 1976, Descriptions of volcanic eruptions, Japan: Bulletin of Volcanological Eruptions, v. 14, no. 43.

Trabant, D.C., 1997, Glacier ice-volume modeling and glacier volumes on Redoubt Volcano, Alaska: U.S. Geological Survey Water-Resources Investigations Report 97-4187, 29 p.

Trabant, D.C., and Meyer, D.F., 1992, Flood generation and destruction of "Drift" glacier by the 1989-90 eruption of Redoubt Volcano, Alaska: Annals of Glaciology, v. 16, p. 33-38.

Trabant, D.C., Waitt, R.B., and Major, J.J., 1994, Disruption of Drift glacier and origin of floods during the 1989-90 eruptions of Redoubt Volcano, Alaska *in* Miller, T.P., and Chouet, B.A., eds., The 1989-1990 eruption of Redoubt Volcano, Alaska: Journal of Volcanology and Geothermal Research, Special Issue, v. 62, no. 1-4, p. 369-385.

Wolfe, E.W., and Pierson, T.C., 1995, Volcanic-hazard zonation for Mount St. Helens, Washington: U.S. Geological Survey Open-File Report 95-497, 12 p.